

CHAPTER III

Parallel responses of bees to past climate change in three isolated archipelagos of the south western Pacific

Scott V. C. Groom ^{a*}, Mark I. Stevens ^{bc}, Michael P. Schwarz ^a

^a *School of Biological Sciences, Flinders University, GPO Box 2100, SA 5001,
Adelaide, Australia*

^b *South Australian Museum, GPO Box 234, SA 5000,*

^c *School of Earth and Environmental Sciences, University of Adelaide, SA 5005,
Adelaide, Australia*

A version of this chapter has been formatted and submitted for publication in:

Proceedings of the Royal Society: Biological Sciences B

Summary

The impacts of glacial cycles on the geographical distribution and size of populations have been explored for numerous terrestrial and marine taxa. However, most studies have focused on high latitudes with few focussed on the response of biota to the last glacial maximum (LGM) in equatorial regions. Here we examine how population sizes of key bee fauna in the south west Pacific archipelagos of Fiji, Vanuatu and Samoa have fluctuated over the Quaternary. We show that all three island faunas suffered massive population declines, roughly corresponding in time to the LGM, followed by rapid expansion post-LGM. Our data therefore suggest that Pleistocene climate change has had major impacts across a very broad tropical region. Whilst other studies indicate widespread Holarctic effects of the LGM, our data suggest a much wider range of latitudes, extending to the tropics, where these climate change repercussions were important. As key pollinators, the inferred changes in these bee faunas may have been critical in the development of the diverse Pacific island flora. The magnitude of these responses indicates future climate change scenarios may have alarming consequences for Pacific island systems involving pollinator-dependent plant communities and agricultural crops.

Keywords: Fiji, Vanuatu, Samoa, Last Glacial Maximum, halictine bees,

Lasioglossum (Homalictus)

1.0 Introduction

Evidence of increases in global average air and ocean temperatures and rising global sea level is widely accepted in the scientific community [1]. Such changes are expected to have varying, and potentially very large, effects on ecosystem composition and function [2]. Potential impacts of climate change on pollinators are important because of their role in angiosperm sexual reproduction [3]. Differing phenological responses between plants and their pollinators to changing climates are particularly concerning [4], yet few empirical studies exist ([5, 6] and references therein).

Short-term responses for some biota to recent climate change can be assessed using museum/herbaria records extending back over the last few hundred years [7].

However, two problems arise when assessing the impact of climate change on plant-pollinator relationships using data that only extend back over recent history: (i) it can be difficult to discriminate between climate change effects *per se* and anthropogenic effects unrelated to climate, such as habitat destruction, introduction of exotics, and pesticide use [8]; and (ii) important changes to plant-pollinator relationships may arise over much longer time-frames [9] or short-term disruptions may be reversed as the affected elements adapt to changed conditions.

One way to explore the effects of climate change on plant-pollinator relationships is to reconstruct phylogenies of the various elements and then to explore diversification patterns and past population sizes. This approach has been used previously to

reconstruct how climate fluctuations impact the population dynamics of both terrestrial and marine organisms; including mammals (*e.g.* [10]) and fish (*e.g.* [11]). Studies of insect populations have also revealed demographic responses to glacial cycles (*e.g.* [12]). However, studies of terrestrial impacts of glacial cycles in tropical islands are scarce, despite their role in understanding island biogeography [13].

Recently, Groom *et al.* [14] examined population size and haplotype accumulation of halictine bees in the genus *Lasioglossum* subgenus *Homalictus* (herein referred to simply as *Homalictus*) in the Fijian archipelago. They argued that there was a decline in population size in the late Holocene, approximately 20 000 ya, followed by a dramatic increase in population size shortly after. They argued that this pattern of decline followed by a rapid bounce-back could be a response to changing climate, with an initially negative reaction to cooling/drying conditions, followed by rapid expansion as global climate reverted to an inter-glacial period. The effects of human transformation of ecosystems was excluded as a confounding effect in their inferred bee demographics because the major increase in historical population size occurred before human occupation of the Fijian archipelago (approximately 3000 years ago). However, there might be other possibilities, unrelated to climate, which could explain the observed patterns. For example, introductions of foreign plant species that provide different food sources, adaptations unrelated to changing climate, or pollinator extinctions leading to filling an available niche. One way to further examine whether climate change really did impact on bee population sizes in tropical islands is to examine changes in bee demographics in other isolated archipelagos of the south west Pacific (SWP).

The south west Pacific has a very depauperate bee fauna [15] and most if not all of the long-tongued bee species in Fiji represent anthropogenic dispersals [16]. The short-tongued *Homalictus* are the most abundant bee element of many of the SWP islands. In Fiji there are four *Homalictus* species [17, 18], six species for the archipelago of Vanuatu [15], and Samoa has the greatest recorded diversity in the SWP with 10 species. Here we use the mitochondrial cytochrome oxidase c subunit I (COI) gene to examine changes in past population sizes of *Homalictus* in three isolated (each separated by at least ~800 km) island archipelagos; Vanuatu, Fiji and Samoa. We explore the timing of bee colonization in each archipelago and use coalescent analyses to explore whether historical demographic changes show patterns that might indicate common responses to historical climate changes in the SWP.

2.0 Material and methods

2.1 Study system

We collected *Homalictus* specimens visiting flowers from three isolated neighbouring archipelagos in the south western Pacific; Vanuatu, Fiji, and Samoa, spanning a total distance of approximately 4000 km (Fig. S1). These island systems have complex and relatively recent geological and volcanic histories, and form highly fragmented island groups. Floral hosts included numerous cosmopolitan and invasive species throughout village gardens, roadsides, and native vegetation, with many flowering year-round. Identifications were based on the species descriptions of Perkins and Cheesman [18], Pauly and Villemant [19], and Michener [17].

2.2 DNA processing

Extraction, amplification and sequencing of mtDNA was performed by the Canadian Centre for DNA Barcoding (CCDB) at the Biodiversity Institute of Ontario using standard protocols [20]. Bidirectional sequencing using the universal primer pair LepF1/LepR2 [21] from a single leg of each specimen produced a 654 bp sequence of COI for 425 *Homalictus* specimens from Fiji, 177 from Vanuatu, and 143 from Samoa. All trace files were examined using Geneious Pro v6.1.6 [22] and haplotypes with one or more ambiguous nucleotide in both forward and reverse directions at the same site were removed from analyses. Identical sequences were also removed, leaving 83 unique haplotypes from Fiji, 30 from Vanuatu, and 41 from Samoa. In total 207 unique haplotypes were aligned, with the 154 Pacific representatives

combined with 53 outgroup Australian species of the closely related *Lasioglossum* subgenus *Chilalictus* and further *Homalictus* sequences obtained via Genbank (see Table S1). The resulting dataset (base frequencies – A: 33.7%, C: 14.3%, G: 11.4%, T: 40.6%) exhibits strong AT bias (74.3%) at the 3rd codon position, as is common in Hymenoptera [23]. To avoid sequence contamination from potential *Wolbachia* infection, sequences were screened using the NCBI BLASTn database. All specimens are stored in the Schwarz Bee Collection at Flinders University, South Australia. Phylogenetic analyses were based on unique COI haplotypes rather than species, and correspondence between the two are discussed below in the Results and Discussion.

2.3 Phylogenetic analyses

Phylogenetic analyses were performed using Bayesian inference implemented in BEAST v. 1.7.5 [29] with an uncorrelated lognormal relaxed molecular clock for 50 million iterations, sampling every 1000th iteration, under a Yule process speciation model. *Chilalictus* was constrained as outgroup with a mean root height of 20 Ma (parameter treeModel.rootHeight normal (mean = 20, s.d. = 3.0)) as per the multi-gene phylogeny of Gibbs et al. [30]. The most suitable substitution prior was determined as GTR + I + Γ by an AIC criterion in jModelTest v.2.1.4, and individual uncorrelated log-normal rate priors set with mean (parameter ucl.d.mean) following an exponential distribution (mean = 0.33, offset = 0) and standard deviation (parameter ucl.d.stdev) followed an exponential distribution (mean = 0.33, offset = 0). Subsequent log files were then examined in Tracer v1.5 to determine if effective sample sizes were adequate (*i.e.* >100). The resulting haplotype tree (Fig. S2) was

compared with an additional genetic-distance based analysis (Fig. S3). Our genetic distance analysis used a neighbour-joining technique applied to uncorrected p-distances in PAUP* v4.0b [26]. Missing gene fragments were not included when calculating pairwise distances, and trees were explored using a heuristic search with 100 random taxon-addition sequence replicates, tree-bisection-reconnection branch swapping, and no limit on the number of shortest trees retained.

2.4 Patterns of haplotype diversification

We explored temporal patterns of haplotype accumulation using log lineage through time (LTT) plots based only on unique haplotypes for each of the three major archipelago clades. One clade representing a second dispersal into Samoa and two other clades, representing later dispersals into Vanuatu (Fig. S2), were not included in the analyses because of the small number of haplotypes recovered from them. We produced LTT plots separately in Tracer v.1.5 for each archipelago based on a Bayesian Skyline coalescent model in BEAST 1.7.5 [24]. After assessing appropriate models using ModelTest, we assigned a GTR + I + Γ substitution model to unpartitioned datasets under a constant rate strict molecular clock of 1.0. Fixing the rate to 1.0, rather than using a relaxed clock, allows the resulting branch lengths to be interpreted in units of mean substitutions per site, which can be converted to years given a mutation rate per generation and the number of generations per year.

2.5 Estimating changes in N_e

To determine whether the observed changes in haplotype accumulation corresponded with shifts in the effective population sizes for the archipelagos, we produced a Bayesian Skyline plot (BSP) for each clade based on the same trees produced for our LTT analyses using a constant-rate fixed strict molecular clock of 1.0 in Tracer v1.5. This produces a tree where branch lengths are proportional to the number of substitutions, and is required to be able to determine node ages based on an estimated number of generations per year. Because our dataset includes representatives from across a wide elevation range (0m to 1100m asl), it is possible that populations at higher elevations have fewer generations per year, and it should be considered that age estimates for these lineages may be underestimated compared to lower elevation populations.

2.6 Dating estimates

There are no documented bee fossils in the Oceania region, and our analyses covered recent divergences, thus calibrating chronogram age estimates is difficult. However, there are other approaches to molecular dating. Few data exist to assess variation in *de novo* mutation rates among taxa [27]. However, two studies have estimated single nucleotide mutation rates for invertebrate mitochondrial genomes; the nematode *Caenorhabditis elegans* [28] and fruit fly *Drosophila melanogaster* [29]. These respective rates were within a single order of magnitude of each other (9.7×10^{-8} and 6.2×10^{-8} per site per generation) and both taxa had AT biases similar to our *Homalictus* dataset (76% and 82% respectively, compared to 74.3% in *Homalictus*). Consequently, a mutation rate in the region of 10^{-8} – 10^{-9} single-nucleotide mutations per generation might be expected for *Homalictus*. Other estimated rates of mutation

in COI of insects were incorporated into divergence date estimates for the bee genus *Bombus*, where Duennes *et al.* [30] applied a rate range of 1.0×10^{-7} to 1.0×10^{-9} substitutions per site per year (one generation per year in *Bombus*). Whilst these estimates differ across two orders of magnitude, they are not adjusted for varying base composition, which can have very strong effects [27]. Consequently, we deemed the *Drosophila* rate of 6.2×10^{-8} per site per generation the most appropriate estimate for our study.

Converting the relative age of nodes based on mutation rates into chronological years requires that we know the number of generations per year for *Homalictus* in our study sites. Unfortunately, the only studies of *Homalictus* nesting biology are those of Knerer & Schwarz [33] on a temperate species from southern Australia which produces two generations per year. Studies on temperate Australian *Lasioglossum* species in the *Lasioglossum* subgenus *Chilalictus* also indicate two generations per year [32]. Although in the tropics Michener & Bennett [33] demonstrate almost year round activity in populations of *Halictus ligatus*, which produced three broods per year. Furthermore, the neotropical halictine *Megalopta genalis* has been shown to have an egg to adult period of approximately 35 days that would allow for up to four generations per year [34]. The number of generations per year in the tropical habitats of the south western Pacific are therefore likely to comprise three as a minimum, but as many as four or more given short egg to adult periods and year round activity.

Using the chronogram produced under the Bayesian Skyline coalescent model analysis above, we were able to estimate; (i) the likely time at which *Homalictus*

arrived in each archipelago, and (ii) the changes in haplotype accumulation and change in effective population size based on key nodes of the tree topology. By setting the number of generations per year, we are able to convert the age of the nodes provided in mutations/site/generation to calendar years.

3.0 Results

Our Bayesian inference analysis indicated a single colonization of Fiji by *Homalictus*, two colonizations of Samoa and three for Vanuatu (Fig. S2). The neighbour-joining analysis (Fig. S3) shows a highly similar topology with clearly monophyletic clades for each of the three Pacific archipelagos, although their arrangement did not agree with our Bayesian approach. The Samoan clade was recovered as sister to the Fijian plus Vanuatu clades. Importantly, the distribution of branch lengths within and between major clades in each archipelago are very similar for these very different tree building approaches, indicating that both topological and diversification patterns in our analyses are robust to very different analytical approaches.

3.1 Haplotype accumulation

Log lineage-through-time (LTT) plots are given for each of the three archipelago clades in Figs 1a-c and are juxtaposed with the corresponding chronograms from our BEAST analysis (Fig. 1g; Fig. S4). Although the number of haplotypes differs within each clade, all three curves share a highly similar shape that increases steadily before rapidly increasing at 5×10^{-3} mutations/site (Fig. S5). The timing of these rapid increases begins at approximately the same time point, which coincides with the emergence of a hyper diverse haplotype clade in the Fijian representatives and the most diverse haplotype clades in the Vanuatu and Samoan clades (Fig. 1g). Considered separately, the changes in haplotype accumulation are striking, and together they suggest parallel temporal responses to a shared stimulus able to influence species over large spatial scales.

3.2 Effective population size

Modelling the effective population size over time using Bayesian skyline plots (Figs 1d-f; Fig. S6) reveals almost identical patterns of change. Again we see largely stable populations over the majority of time but a dramatic drop in N_e occurs at approximately 5.0×10^{-3} mutations/site before a large increase at 2.5×10^{-3} mutations/site. Aligning the scales of our BSPs and chronograms indicate these changes appear to occur within a very similar time frame, and the tree topologies (Fig. 1g) demonstrate that this timing corresponds to both a sudden decrease and then sudden increase in N_e across each of the archipelagos.

3.3 Age estimates

We were able to determine the approximate ages of two key components of our plots by applying the single nucleotide mutation rate [29], and our estimated number of generations per year. Firstly, based on node ages of 0.1322, 0.0999, and 0.051 mutations/site and four generations per year, we obtain crown age estimates of 533 kya, 403 kya, and 206 kya for Vanuatu, Fiji and Samoa, respectively. If we instead assume three generations per year the estimates increase to 711 kya, 537 kya, 274 kya for Vanuatu, Fiji and Samoa, respectively. These various ages are only a fraction of the islands respective geological ages of 3 – 8 Mya [35], 12.5 – 29 Mya [36], and 5 Mya [37]. Secondly, by aligning our resulting tree topologies with both LTT and Bayesian skyline plots we determined that both the increase in haplotype accumulation and change in N_e occurred at approximately 0.006 mutations/site.

Based on four generations per year this equates to 24 kya, or approximately 32 kya based if three generations per year are assumed. This suggests a stimulus or stimuli common across all three isolated island groups. Likewise, if the increase in N_e occurred at 0.0025 mutations/site, the estimated onset of increasing N_e is approximately 10 kya based on four generations per year, or 13 kya based on three generations. Based on these estimates, the changes presented in N_e appear broadly concordant with a major global change in the last glacial termination (Fig. 1h).

4.0 Discussion

Numerous studies have outlined the effects of glacial cycles on Palearctic and Nearctic biota, with contractions to southern refugia during glacial maxima and then subsequent northern expansions following deglaciation [38]. Less detailed studies have inferred similar patterns in the southern hemisphere [39] but few have examined how biota in tropical latitudes have responded to these global cycles (*e.g.* [40]). The tropical Pacific represents a major driving force behind current global climates, and is expected to have played a considerable role throughout glacial periods [41]. Despite its importance, reconstruction of climatic variation in the region over time has been limited by short or insufficiently resolved records, and confidence in extrapolating data from neighbouring regions is therefore similarly limited.

We found that the principal bee fauna in three major south west Pacific archipelagos, spanning a distance of approximately 4000 km and representing multiple colonization events but with no subsequent interchanges, show remarkably similar patterns of haplotype accumulation since the late Pleistocene. Our LTT plots suggest marked anti-sigmoidal patterns for haplotype accumulation in the *Homalictus* fauna from Fiji, Vanuatu and Samoa, and our phylogenetic analyses indicate that these similarities cannot be explained by dispersal events linking the bee faunas in these regions. Consequently, *Homalictus* bees in these regions appear to have independently responded to some factor(s) influencing each of the archipelagos, and any such factor(s) seem to have operated within a close timeframe for each

archipelago. For any such factor(s) to have impacted over such a large geographic scale there are few likely explanations.

Anti-sigmoidal LTT plots can arise from both 3-phase Yule models of radiation as well as from major extinction events [42], and it can be very difficult to discriminate between these alternatives [43]. However, our BSP analyses clearly indicate major declines in effective population sizes of *Homalictus* for each of the three archipelagos at approximately the same time point. Although single locus demographic reconstructions are limited in their confidence with increasing time [44], very recent timescales ensure strong phylogenetic signal for conspecific variation and render the impact of saturation on our analyses negligible. Instead, confidence in estimating this time point is limited due to potential variation in the applied mutation rate and generations per year, yet all likely scenarios commonly indicate the decrease and subsequent increase occurred either side of the last glacial maximum (LGM). The LGM involved both global cooling as well as considerable decreases in precipitation for widely separated regions neighbouring the SWP, including Australia [45], Borneo [46] and Chile [47]. Such conditions have been shown to have influenced similar contraction/expansion population dynamics in the goby fish of the SWP due to sea level fluctuations, determined via deep sea sediment cores [48]. However, the impacts on terrestrial biota on this region have not been well explored.

A recent study of Borneo stalagmite $\delta^{18}\text{O}$ records provides the closest comparison for the possible SWP climate variation and demonstrates a 100 ky glacial-interglacial

cycle throughout the Quaternary with a clear increase in atmospheric moisture since the LGM [46]. Palynology studies of the highland Lake Tagamaucia in Fiji [49] and Lynch's Crater in north east Australia [45] indicate a distinct change in vegetation composition beginning approximately 15 kya during a marked post-LGM warming period. With these exceptions, very few studies have attempted to reconstruct SWP climates across the LGM, so the impact of climate change in this region remains largely unexplored.

Our results suggest that some factor(s) forced near-simultaneous changes in bee populations across a wide region of the SWP. We are unable to say whether these changes are due to climate directly forcing changes in bee populations, indirect effects arising from changes in angiosperm communities, or a mixture of both. However, because bees are key pollinators in terrestrial ecosystems, it seems very likely that our inferred fluctuations in bee demography will have had very broad impacts. Island systems often harbour low species richness, which can result in a broadened range of host plant species for pollinators due to reduced competition resulting in keystone 'super generalist' species [50]. This seems very likely for Fiji, Vanuatu and Samoa, where most, if not all, non-*Homalictus* bees are likely to represent post-LGM and/or anthropogenic arrivals [16, 51].

If the changes in bee populations that we infer here involve corresponding changes in angiosperm communities, either via shared forcing events or effects on pollinator abundance, then events surrounding the LGM are likely to have broadly impacted tropical island ecosystems as well as the better-understood Palearctic and Nearctic

biota. Given predicted climate change scenarios, studies are needed to determine how climate change may impact pollinator dependent plant communities including agricultural crops. As tropical ecosystems are major sources of biodiversity, incorporating a large proportion of the developing world, the consequences of disrupting plant pollinator interactions could be considerable.

5.0 Acknowledgements

We thank all members of the South Pacific Regional Herbarium at the University of the South Pacific, in particular Marika Tuiwawa and Alivereti Naikatini, for their invaluable assistance with Fijian field logistics and expertise. Vanuatu collections would not have been possible without the assistance of Linette Birukilukilu and Plant Health and Quarantine who oversaw remote field collections and facilitated permit acquisition in Vanuatu. The support of Afele Faiilagi and the Ministry for Natural Resources and Environment enabled sampling to be conducted in Samoa. This research was possible thanks to the financial support of the Australia Pacific Science Foundation, Rufford Foundation, National Climate Change Adaptation Research Facility, and an Australia Awards Endeavour Research Fellowship awarded to SVCG.

Data Accessibility

DNA sequences may be accessed via corresponding Genbank Accession or BOLD ID numbers listed for all included specimens in Supplementary Table 1.

6.0 References

1. IPCC. 2007 Climate Change 2007: The Physical Science Basis. Contribution of Working Group I to the Fourth Assessment Report of the Intergovernmental Panel on Climate Change. Cambridge, United Kingdom and New York, NY, USA., Cambridge University Press.
2. Thomas C.D., Cameron A., Green R.E., Bakkenes M., Beaumont L.J., Collingham Y.C., Erasmus B.F.N., de Siqueira M.F., Grainger A., Hannah L., et al. 2004 Extinction risk from climate change. *Nature* 427(6970), 145-148. (doi:10.1038/Nature02121).
3. Kremen C., Williams N.M., Aizen M.A., Gemmill-Herren B., LeBuhn G., Minckley R., Packer L., Potts S.G., Roulston T., Steffan-Dewenter I., et al. 2007 Pollination and other ecosystem services produced by mobile organisms: a conceptual framework for the effects of land-use change. *Ecol Lett* 10(4), 299-314. (doi:10.1111/J.1461-0248.2007.01018.X).
4. Rafferty N.E., Ives A.R. 2011 Effects of experimental shifts in flowering phenology on plant-pollinator interactions. *Ecol Lett* 14(1), 69-74. (doi:10.1111/J.1461-0248.2010.01557.X).
5. Hegland S.J., Nielsen A., Lazaro A., Bjerknes A.L., Totland O. 2009 How does climate warming affect plant-pollinator interactions? *Ecol Lett* 12(2), 184-195. (doi:10.1111/J.1461-0248.2008.01269.X).
6. Willmer, P. 2012 Ecology: pollinator–plant synchrony tested by climate change. *Current Biol* 22(4), R131-R132.
7. Cameron S.A., Lozier J.D., Strange J.P., Koch J.B., Cordes N., Solter L.F., Griswold T.L. 2011 Patterns of widespread decline in North American bumble bees. *P Natl Acad Sci USA* 108(2), 662-667. (doi:10.1073/Pnas.1014743108).
8. Schweiger O., Biesmeijer J.C., Bommarco R., Hickler T., Hulme P.E., Klotz S., Kuhn I., Moora M., Nielsen A., Ohlemuller R., et al. 2010 Multiple stressors on biotic interactions: how climate change and alien species interact to affect pollination. *Biol Rev* 85(4), 777-795. (doi:10.1111/J.1469-185x.2010.00125.X).
9. Bartomeus I., Ascher J.S., Gibbs J., Danforth B.N., Wagner D.L., Hedtke S.M., Winfree R. 2013 Historical changes in northeastern US bee pollinators related to shared ecological traits. *P Natl Acad Sci USA* 110(12), 4656-4660. (doi:10.1073/Pnas.1218503110).
10. Palkopoulou E., Dalén L., Lister A.M., Vartanyan S., Sablin M., Sher A., Edmark V.N., Brandström M.D., Germonpré M., Barnes I., et al. 2013 Holarctic genetic structure and range dynamics in the woolly mammoth. *Proceedings of the Royal Society B: Biological Sciences* 280(1770). (doi:10.1098/rspb.2013.1910).
11. Ruzzante D.E., Walde S.J., Gosse J.C., Cussac V.E., Habit E., Zemplak T.S., Adams E.D.M. 2008 Climate control on ancestral population dynamics: insight from Patagonian fish phylogeography. *Mol Ecol* 17(9), 2234-2244. (doi:10.1111/J.1365-294x.2008.03738.X).

12. Buckley T.R., Marske K.A., Attanayake D. 2009 Identifying glacial refugia in a geographic parthenogen using palaeoclimate modelling and phylogeography: the New Zealand stick insect *Argosarchus horridus* (White). *Mol Ecol* 18(22), 4650-4663. (doi:10.1111/J.1365-294x.2009.04396.X).
13. Whittaker R.J., Fernandez-Palacios J.M. 2007 *Island biogeography: ecology, evolution, and conservation*. 2nd ed. Oxford, Oxford University Press.
14. Groom S.V.C., Stevens M.I., Schwarz M.P. 2013 Diversification of Fijian halictine bees: Insights into a recent island radiation. *Mol Phylogenet Evol* 68(3), 582-594. (doi:10.1016/J.Ympev.2013.04.015).
15. Groom S.V.C., Schwarz M.P. 2011 Bees in the Southwest Pacific: Origins, diversity and conservation. *Apidologie* 42(6), 759-770. (doi:10.1007/S13592-011-0079-8).
16. Davies O., Groom S.V.C., Ngo H.T., Stevens M.I., Schwarz M.P. 2013 Diversity and Origins of Fijian Leaf-Cutter Bees (Megachilidae). *Pacific Science* 67(4), 561-570.
17. Michener C.D. 1979 Genus *Homalictus* in Fiji (Hymenoptera, Halictidae). *Pac Insects* 21(2-3), 227-234.
18. Perkins R.C.L., Cheesman L.E. 1928 Hymenoptera - Apoidea, Sphecoidea, and Vespoidea. *Insects of Samoa Part V.(Fasc. 1)*, 1-32.
19. Pauly A., Villemant C. 2009 Hyménoptères Apoidea (Insecta) de l'archipel du Vanuatu. *Zoosystema* 31(3), 719-730.
20. Ivanova N.V., Dewaard J.R., Hebert P.D.N. 2006 An inexpensive, automation-friendly protocol for recovering high-quality DNA. *Mol Ecol Notes* 6(4), 998-1002. (doi:10.1111/J.1471-8286.2006.01428.X).
21. Hebert P.D.N., Penton E.H., Burns J.M., Janzen D.H., Hallwachs W. 2004 Ten species in one: DNA barcoding reveals cryptic species in the neotropical skipper butterfly *Astraptes fulgerator*. *P Natl Acad Sci USA* 101(41), 14812-14817. (doi:10.1073/Pnas.0406166101).
22. Drummond A., Ashton B., Buxton S., Cheung M., Cooper A., Duran C., Field M., Heled J., Kearse M., Markowitz S., et al. 2012 *Geneious*. v.5.6.4
23. Schwarz M.P., Tierney S.M., Cooper S.J.B., Bull N.J. 2004 Molecular phylogenetics of the allodapine bee genus *Braunsapis*: A-T bias and heterogeneous substitution parameters. *Mol Phylogenet Evol* 32, 110-122.
24. Drummond A.J., Rambaut A. 2007 BEAST: Bayesian evolutionary analysis by sampling trees. *Bmc Evol Biol* 7. (doi:10.1186/1471-2148-7-214).
25. Gibbs J., Brady S.G., Kanda K., Danforth B.N. 2012 Phylogeny of halictine bees supports a shared origin of eusociality for *Halictus* and *Lasioglossum* (Apoidea: Anthophila: Halictidae). *Mol Phylogenet Evol* 65(3), 926-939. (doi:10.1016/J.Ympev.2012.08.013).

26. Swofford D.L. 1999 PAUP. Phylogenetic analysis using parsimony (*and other methods). (Sunderland, Massachusetts, Sinauer Associates).
27. Montooth K.L., Rand D.M. 2008 The spectrum of mitochondrial mutation differs across species. *Plos Biol* 6(8), 1634-1637. (doi:10.1371/journal.pbio.0060213).
28. Denver D.R., Morris K., Lynch M., Vassilieva L.L., Thomas W.K. 2000 High direct estimate of the mutation rate in the mitochondrial genome of *Caenorhabditis elegans*. *Science* 289(5488), 2342-2344.
29. Haag-Liautard C., Coffey N., Houle D., Lynch M., Charlesworth B., Keightley P.D. 2008 Direct estimation of the mitochondrial DNA mutation rate in *Drosophila melanogaster*. *Plos Biol* 6(8), 1706-1714. (doi:10.1371/journal.pbio.0060204).
30. Duennes M.A., Lozier J.D., Hines H.M., Cameron S.A. 2012 Geographical patterns of genetic divergence in the widespread Mesoamerican bumble bee *Bombus ephippiatus* (Hymenoptera: Apidae). *Mol Phylogenet Evol* 64(1), 219-231. (doi:10.1016/J.Ympev.2012.03.018).
31. Knerer G., Schwarz M.P. 1976 Halictine Social Evolution: The Australian Enigma. *Science* 194(445), 445-448.
32. Kukuk P.F. 2002 Nest reuse in a communal halictine bee, *Lasioglossum (Chilalictus) hemichalceum* (Hymenoptera : Halictidae). *J Kansas Entomol Soc* 75(1), 3-7.
33. Michener C.D., Bennett F.D. 1977 Geographical variation in nesting biology and social organization of *Halictus ligatus*. *University of Kansas Science Bulletin* 51, 233-260
34. Wcislo W.T., Arneson L., Roesch K., Gonzalez V., Smith A., Fernandez H. 2004 The evolution of nocturnal behaviour in sweat bees, *Megalopta genalis* and *M. ecuadoria* (Hymenoptera : Halictidae): an escape from competitors and enemies? *Biol J Linn Soc* 83(3), 377-387. (doi:10.1111/J.1095-8312.2004.00399.X).
35. Crawford A., Meffre S., Symonds P. 2003 120 to 0 Ma tectonic evolution of the southwest Pacific and analogous geological evolution of the 600 to 220 Ma Tasman Fold Belt System. *Special Papers - Geological Society of America*, 383-404.
36. Taylor G.K., Gascoyne J., Colley H. 2000 Rapid rotation of Fiji: Paleomagnetic evidence and tectonic implications. *J Geophys Res-Sol Ea* 105(B3), 5771-5781. (doi:10.1029/1999jb900305).
37. Hart S.R., Coetzee M., Workman R.K., Blusztajn J., Johnson K.T.M., Sinton J.M., Steinberger B., Hawkins J.W. 2004 Genesis of the Western Samoa seamount province: age, geochemical fingerprint and tectonics. *Earth Planet Sc Lett* 227(1-2), 37-56. (doi:10.1016/J.Epsl.2004.08.005).
38. Hewitt G. 2000 The genetic legacy of the Quaternary ice ages. *Nature* 405(6789), 907-913. (doi:10.1038/35016000).

39. McGaughran A., Stevens M.I., Holland B.R. 2010 Biogeography of circum-Antarctic springtails. *Mol Phylogenet Evol* 57(1), 48-58. (doi:10.1016/J.Ympev.2010.06.003).
40. Colinvaux P.A., De Oliveira P.E. 2001 Amazon plant diversity and climate through the Cenozoic. *Palaeogeography, Palaeoclimatology, Palaeoecology* 166(1-2), 51-63. (doi:http://dx.doi.org/10.1016/S0031-0182(00)00201-7).
41. Kienast M., Kienast S.S., Calvert S.E., Eglinton T.I., Mollenhauer G., Francois R., Mix A.C. 2006 Eastern Pacific cooling and Atlantic overturning circulation during the last deglaciation. *Nature* 443(7113), 846-849. (doi:http://www.nature.com/nature/journal/v443/n7113/supinfo/nature05222_S1.html).
42. Crisp M.D., Cook L.G. 2009 Explosive radiation or cryptic mass extinction? Interpreting signatures in molecular phylogenies. *Evolution* 63(9), 2257-2265. (doi:10.1111/j.1558-5646.2009.00728.x).
43. Rehan S.M., Leys R., Schwarz M.P. 2013 First Evidence for a Massive Extinction Event Affecting Bees Close to the K-T Boundary. *Plos One* 8(10). (doi:10.1371/journal.pone.0076683).
44. Gill M.S., Lemey P., Faria N.R., Rambaut A., Shapiro B., Suchard M.A. 2012 Improving Bayesian Population Dynamics Inference: A Coalescent-Based Model for Multiple Loci. *Molecular Biology and Evolution*. (doi:10.1093/molbev/mss265).
45. Muller J., Kylander M., Wust R.A.J., Weiss D., Martinez-Cortizas A., LeGrande A.N., Jennerjahn T., Behling H., Anderson W.T., Jacobson G. 2008 Possible evidence for wet Heinrich phases in tropical NE Australia: the Lynch's Crater deposit. *Quaternary Sci Rev* 27(5-6), 468-475. (doi:10.1016/J.Quascirev.2007.11.006).
46. Meckler A.N., Clarkson M.O., Cobb K.M., Sodemann H., Adkins J.F. 2012 Interglacial Hydroclimate in the Tropical West Pacific Through the Late Pleistocene. *Science* 336(6086), 1301-1304. (doi:10.1126/Science.1218340).
47. Denton G.H., Heusser C., Lowel T., Moreno P.I., Andersen B.G., Heusser L.E., Schlüchter C., Marchant D.R. 1999 Interhemispheric linkage of paleoclimate during the last glaciation. *Geografiska Annaler: Series A, Physical Geography* 81(2), 107-153.
48. Hoareau T.B., Boissin E., Berrebi P. 2012 Evolutionary history of a widespread Indo-Pacific goby: The role of Pleistocene sea-level changes on demographic contraction/expansion dynamics. *Mol Phylogenet Evol* 62(1), 566-572. (doi:10.1016/J.Ympev.2011.10.004).
49. Hope G., Stevenson J., Southern W. 2009 Vegetation histories from the Fijian Islands: Alternative records of human impact [in] *The early prehistory of Fiji* [electronic resource]. Canberra, Australia, ANU E Press.

50. Olesen J.M., Eskildsen L.I., Venkatasamy S. 2002 Invasion of pollination networks on oceanic islands: importance of invader complexes and endemic super generalists. *Divers Distrib* 8(3), 181-192.
51. Groom S.V.C., Ngo H.T., Rehan S.M., Stevens M.I., Schwarz M.P. 2014 Multiple recent introductions of apid bees into Pacific archipelagos signify potentially large consequences for both agriculture and indigenous ecosystems. *Biol Invasions* [Early Online] (doi:10.1007/s10530-014-0664-7)

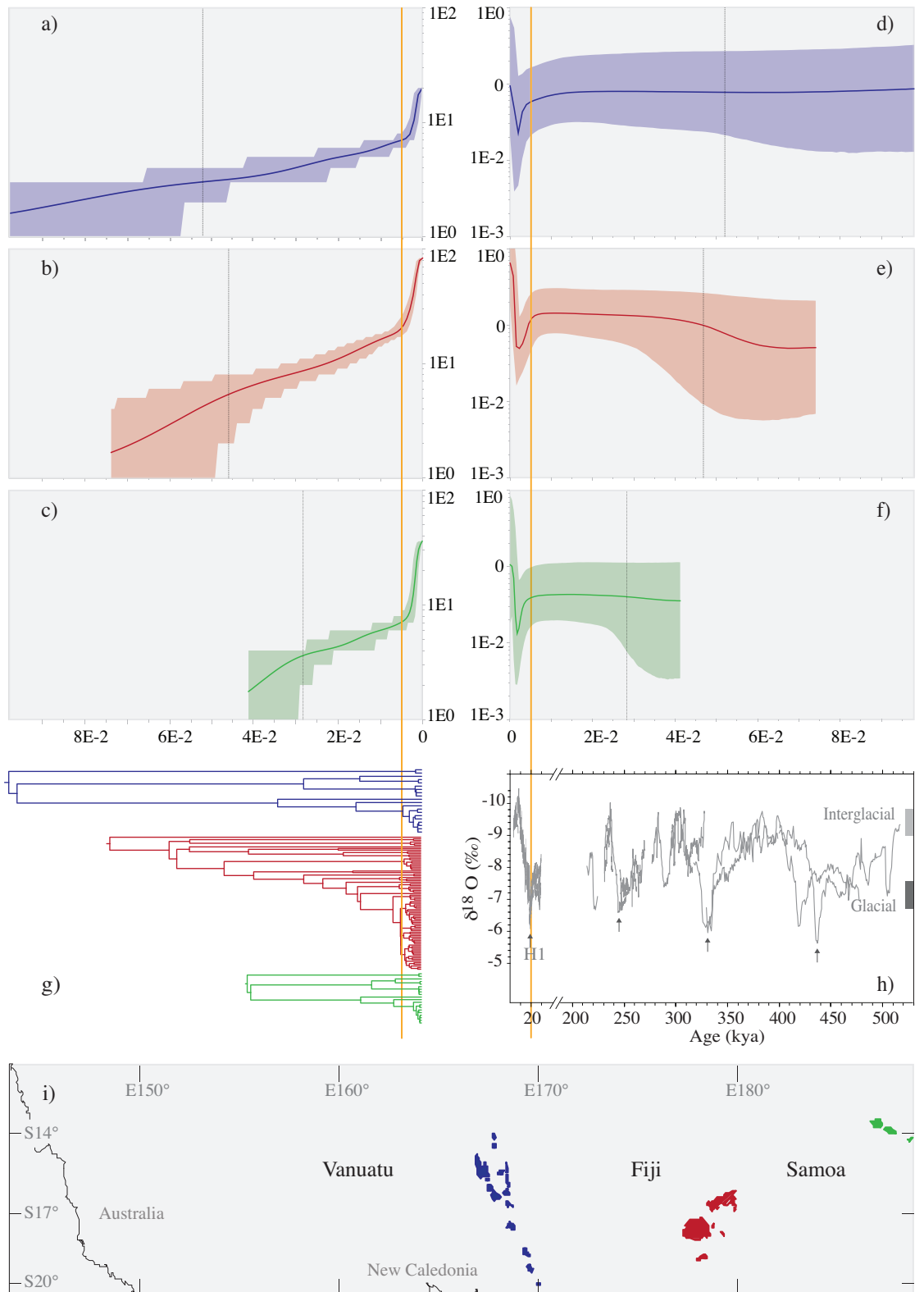


Figure 1. (a-c) Log lineage through time (LTT) plots based on Bayesian skyline chronograms with an enforced strict clock rate of 1.0 implemented in Tracer v1.5. X-axis is presented in units of mutations per site. Maximum times is the root height mean, dotted vertical line represents lower 95% highest posterior density. Each plot colour coded to corresponding archipelago; (d-f) Corresponding Bayesian skyline plot (BSP) for each data file of Fig. 1a-c representing colour coded archipelagos. Bold coloured plot line indicates mean plot values; shaded area represents upper and lower confidence intervals for mean estimates. The y-axis can be interpreted as N_e mutation rate/site, and if mutations rates are assumed to be constant, this can be interpreted as a measure of relative N_e over time. The x-axis is given in units of mutations per site; (g) Maximum credibility trees corresponding to archipelago data files of Fig. 1a-f implemented via BEAST with a strict molecular clock, fixed to 1.0, and Bayesian skyline speciation model. Orange vertical line indicates tree topology corresponding to key changes in LTT plot shape. (h) Borneo stalagmite $\delta^{18}\text{O}$ records. Figure adapted from Meckler et al. (2012) to indicate the published record for the last glacial termination from this location, H1 indicates Heinrich event 1. Age markers are shown along x-axis. Light and dark gray bars on the right show range of interglacial and glacial values, respectively, and black arrows highlight $\delta^{18}\text{O}$ maxima interpreted as deglacial drying phases. Orange vertical line indicates last glacial termination corresponding to key changes in effective population size (N_e); (i) Map indicating sampling areas with longitude and latitude values provided. Archipelagos colour coded to preceding plots as follows; Vanuatu = blue, Fiji = red, Samoa = green.

Table S1. Locality data for species included in the data set. Specimen ID indicates BOLD ID numbers unless underlined, which indicates GenBank accessions.

Specimen ID	Species	Country	State/Island	Lat	Lon
<u>JQ266386</u>	<i>L. (Chilalictus) baudini</i>	Australia	Vic	-	-
<u>JQ266390</u>	<i>L. (Chilalictus) calophyllae</i>	Australia	NSW	-	-
<u>JQ266387</u>	<i>L. (Chilalictus) chapmani</i>	Australia	Vic	-	-
<u>AF103951</u>	<i>L. (Chilalictus) convexum</i>	Australia	Vic	-	-
<u>AF103954</u>	<i>L. (Chilalictus) erythrurum</i>	Australia	SA	-	-
<u>JQ266391</u>	<i>L. (Chilalictus) fasciatum</i>	Australia	SA	-	-
<u>AF103955</u>	<i>L. (Chilalictus) florale</i>	Australia	SA	-	-
MSAPB1252-12	<i>L. (Chilalictus) sp.</i>	Australia	SA	-30.1595	131.581
MSAPB1293-12	<i>L. (Chilalictus) sp.</i>	Australia	Qld	-20.7245	139.495
MSAPB847-11	<i>L. (Chilalictus) sp.</i>	Australia	NT	-15.582	133.22
<u>JQ266402</u>	<i>L. (Chilalictus) supralucens</i>	Australia	WA	-	-
MSAPB846-11	<i>L. (Homalictus) bremerensis</i>	Australia	NT	-14.896	133.038
MSAPB854-11	<i>L. (Homalictus) bremerensis</i>	Australia	Qld	-17.274	145.582
MSAPB855-11	<i>L. (Homalictus) bremerensis</i>	Australia	Qld	-18.252	146.005
<u>JQ266442</u>	<i>L. (Homalictus) holochlorum</i>	Australia	Vic	-	-
MSAPB1212-12	<i>L. (Homalictus) holochlorum</i>	Australia	WA	-18.9801	126.064
MSAPB1219-12	<i>L. (Homalictus) holochlorum</i>	Australia	WA	-17.9512	122.244
MSAPB1220-12	<i>L. (Homalictus) holochlorum</i>	Australia	WA	-17.9512	122.244
MSAPB1231-12	<i>L. (Homalictus) holochlorum</i>	Australia	WA	-18.2112	127.682
MSAPB1247-12	<i>L. (Homalictus) holochlorum</i>	Australia	WA	-17.9512	122.244
MSAPB851-11	<i>L. (Homalictus) houstoni</i>	Australia	NT	-14.896	133.038
<u>JQ266443</u>	<i>L. (Homalictus) megastigmus</i>	Australia	WA	-	-
MSAPB852-11	<i>L. (Homalictus) murrayi</i>	Australia	WA	-34.981	117.426
MSAPB850-11	<i>L. (Homalictus) scrupulosum</i>	Australia	NT	-15.34	133.151
ASBEE095-08	<i>L. (Homalictus) sp.</i>	Australia	Vic	-	-
AUSBC2013-12	<i>L. (Homalictus) sp.</i>	Australia	SA	-33.979	140.953
BEECF258-10	<i>L. (Homalictus) sp.</i>	Australia	Qld	-17.3	145.47
BEECF259-10	<i>L. (Homalictus) sp.</i>	Australia	Qld	-17.3	145.47
BEECF261-10	<i>L. (Homalictus) sp.</i>	Australia	Qld	-17.3	145.47
BEECF264-10	<i>L. (Homalictus) sp.</i>	Australia	Qld	-17.3	145.47
BOTWA1785-12	<i>L. (Homalictus) sp.</i>	Australia	Qld	-27.499	142.623
BOTWA1787-12	<i>L. (Homalictus) sp.</i>	Australia	Qld	-27.499	142.623
BOTWA1788-12	<i>L. (Homalictus) sp.</i>	Australia	Qld	-27.499	142.623
BOTWA1791-12	<i>L. (Homalictus) sp.</i>	Australia	Qld	-27.499	142.623
BOWAU059-10	<i>L. (Homalictus) sp.</i>	Australia	Qld	-17.3	145.47
BOWAU162-11	<i>L. (Homalictus) sp.</i>	Australia	WA	-33.9574	119.915
HYQT283-09	<i>L. (Homalictus) sp.</i>	Australia	Qld	-19.2828	146.801
HYQTB281-12	<i>L. (Homalictus) sp.</i>	Australia	Qld	-19.283	146.801
HYQTB291-12	<i>L. (Homalictus) sp.</i>	Australia	Qld	-19.283	146.801
HYQTB308-12	<i>L. (Homalictus) sp.</i>	Australia	Qld	-19.283	146.801
MSAPB1199-12	<i>L. (Homalictus) sp.</i>	Australia	WA	-17.9512	122.244
MSAPB1203-12	<i>L. (Homalictus) sp.</i>	Australia	Vic	-38.3464	141.604
MSAPB1217-12	<i>L. (Homalictus) sp.</i>	Australia	WA	-18.2241	127.668
MSAPB1218-12	<i>L. (Homalictus) sp.</i>	Australia	WA	-18.2241	127.668
MSAPB1224-12	<i>L. (Homalictus) sp.</i>	Australia	NT	-14.9249	133.069
MSAPB1226-12	<i>L. (Homalictus) sp.</i>	Australia	NT	-14.9249	133.069
MSAPB1227-12	<i>L. (Homalictus) sp.</i>	Australia	SA	-34.7359	140.512
MSAPB1239-12	<i>L. (Homalictus) sp.</i>	Australia	Qld	-20.7245	139.495
MSAPB1241-12	<i>L. (Homalictus) sp.</i>	Australia	Qld	-20.7245	139.495
MSAPB1248-12	<i>L. (Homalictus) sp.</i>	Australia	SA	-30.1595	131.581
<u>JQ266445</u>	<i>L. (Homalictus) sphecodoides</i>	Australia	SA	-	-
MSAPB849-11	<i>L. (Homalictus) urbanum</i>	Australia	NT	-15.34	133.151
MSAPB1188-12	<i>L. (Homalictus) achrostus</i>	Fiji	Viti Levu	-17.5762	177.935
MSAPB032-11	<i>L. (Homalictus) fjiensis</i>	Fiji	Viti Levu	-18.151	178.441
MSAPB035-11	<i>L. (Homalictus) fjiensis</i>	Fiji	Viti Levu	-18.151	178.441
MSAPB062-11	<i>L. (Homalictus) fjiensis</i>	Fiji	Viti Levu	-18.15	178.453
MSAPB1005-12	<i>L. (Homalictus) fjiensis</i>	Fiji	Ono-i-Lau	-20.607	-178.682
MSAPB1006-12	<i>L. (Homalictus) fjiensis</i>	Fiji	Ono-i-Lau	-20.607	-178.682
MSAPB1014-12	<i>L. (Homalictus) fjiensis</i>	Fiji	Namuka-i-Lau	-18.8493	-178.669
MSAPB1015-12	<i>L. (Homalictus) fjiensis</i>	Fiji	Namuka-i-Lau	-18.8493	-178.669
MSAPB1018-12	<i>L. (Homalictus) fjiensis</i>	Fiji	Vuloga	-19.1509	-178.58
MSAPB1023-12	<i>L. (Homalictus) fjiensis</i>	Fiji	Kabara	-18.9353	-178.957

MSAPB1026-12	<i>L. (Homalictus) fijiensis</i>	Fiji	Kabara	-18.9353	-178.957
MSAPB1027-12	<i>L. (Homalictus) fijiensis</i>	Fiji	Totoya	-18.9681	-179.883
MSAPB1028-12	<i>L. (Homalictus) fijiensis</i>	Fiji	Totoya	-18.9681	-179.883
MSAPB1030-12	<i>L. (Homalictus) fijiensis</i>	Fiji	Totoya	-18.9681	-179.883
MSAPB1031-12	<i>L. (Homalictus) fijiensis</i>	Fiji	Totoya	-18.9681	-179.883
MSAPB1034-12	<i>L. (Homalictus) fijiensis</i>	Fiji	Matuku	-19.1504	179.75
MSAPB1040-12	<i>L. (Homalictus) fijiensis</i>	Fiji	Vanua Vatu	-18.3751	-179.27
MSAPB1042-12	<i>L. (Homalictus) fijiensis</i>	Fiji	Moala	-18.5583	179.929
MSAPB1044-12	<i>L. (Homalictus) fijiensis</i>	Fiji	Moala	-18.5583	179.929
MSAPB1045-12	<i>L. (Homalictus) fijiensis</i>	Fiji	Moala	-18.5617	179.928
MSAPB1165-12	<i>L. (Homalictus) fijiensis</i>	Fiji	Moala	-18.5617	179.928
MSAPB1173-12	<i>L. (Homalictus) fijiensis</i>	Fiji	Taveuni	-16.8261	-179.989
MSAPB149-11	<i>L. (Homalictus) fijiensis</i>	Fiji	Vanua Levu	-16.434	179.363
MSAPB151-11	<i>L. (Homalictus) fijiensis</i>	Fiji	Vanua Levu	-16.434	179.363
MSAPB191-11	<i>L. (Homalictus) fijiensis</i>	Fiji	Viti Levu	-18.247	178.08
MSAPB209-11	<i>L. (Homalictus) fijiensis</i>	Fiji	Viti Levu	-18.247	178.08
MSAPB222-11	<i>L. (Homalictus) fijiensis</i>	Fiji	Viti Levu	-18.233	177.79
MSAPB258-11	<i>L. (Homalictus) fijiensis</i>	Fiji	Viti Levu	-17.422	177.996
MSAPB271-11	<i>L. (Homalictus) fijiensis</i>	Fiji	Viti Levu	-17.404	177.782
MSAPB293-11	<i>L. (Homalictus) fijiensis</i>	Fiji	Viti Levu	-17.52	177.925
MSAPB295-11	<i>L. (Homalictus) fijiensis</i>	Fiji	Viti Levu	-17.52	177.925
MSAPB298-11	<i>L. (Homalictus) fijiensis</i>	Fiji	Viti Levu	-17.52	177.925
MSAPB307-11	<i>L. (Homalictus) fijiensis</i>	Fiji	Viti Levu	-17.549	177.943
MSAPB326-11	<i>L. (Homalictus) fijiensis</i>	Fiji	Viti Levu	-17.612	177.986
MSAPB331-11	<i>L. (Homalictus) fijiensis</i>	Fiji	Viti Levu	-17.612	177.986
MSAPB332-11	<i>L. (Homalictus) fijiensis</i>	Fiji	Viti Levu	-17.612	177.986
MSAPB348-11	<i>L. (Homalictus) fijiensis</i>	Fiji	Viti Levu	-17.727	178.084
MSAPB350-11	<i>L. (Homalictus) fijiensis</i>	Fiji	Kadavu	-17.773	178.127
MSAPB353-11	<i>L. (Homalictus) fijiensis</i>	Fiji	Kadavu	-19.047	178.165
MSAPB355-11	<i>L. (Homalictus) fijiensis</i>	Fiji	Kadavu	-19.047	178.165
MSAPB357-11	<i>L. (Homalictus) fijiensis</i>	Fiji	Kadavu	-19.042	178.17
MSAPB359-11	<i>L. (Homalictus) fijiensis</i>	Fiji	Kadavu	-19.042	178.17
MSAPB361-11	<i>L. (Homalictus) fijiensis</i>	Fiji	Kadavu	-19.042	178.17
MSAPB369-11	<i>L. (Homalictus) fijiensis</i>	Fiji	Kadavu	-19.038	178.17
MSAPB371-11	<i>L. (Homalictus) fijiensis</i>	Fiji	Kadavu	-19.038	178.17
MSAPB373-11	<i>L. (Homalictus) fijiensis</i>	Fiji	Kadavu	-19.038	178.17
MSAPB374-11	<i>L. (Homalictus) fijiensis</i>	Fiji	Kadavu	-19.038	178.17
MSAPB385-11	<i>L. (Homalictus) fijiensis</i>	Fiji	Kadavu	-19.046	178.162
MSAPB388-11	<i>L. (Homalictus) fijiensis</i>	Fiji	Kadavu	-19.046	178.162
MSAPB389-11	<i>L. (Homalictus) fijiensis</i>	Fiji	Kadavu	-19.046	178.162
MSAPB392-11	<i>L. (Homalictus) fijiensis</i>	Fiji	Kadavu	-18.953	178.378
MSAPB406-11	<i>L. (Homalictus) fijiensis</i>	Fiji	Kadavu	-18.957	178.375
MSAPB457-11	<i>L. (Homalictus) fijiensis</i>	Fiji	Kadavu	-18.987	178.475
MSAPB460-11	<i>L. (Homalictus) fijiensis</i>	Fiji	Kadavu	-18.987	178.475
MSAPB462-11	<i>L. (Homalictus) fijiensis</i>	Fiji	Kadavu	-18.97	178.428
MSAPB463-11	<i>L. (Homalictus) fijiensis</i>	Fiji	Kadavu	-18.97	178.428
MSAPB472-11	<i>L. (Homalictus) fijiensis</i>	Fiji	Vanua Levu	-16.43	179.373
MSAPB473-11	<i>L. (Homalictus) fijiensis</i>	Fiji	Vanua Levu	-16.43	179.373
MSAPB474-11	<i>L. (Homalictus) fijiensis</i>	Fiji	Vanua Levu	-16.43	179.373
MSAPB475-11	<i>L. (Homalictus) fijiensis</i>	Fiji	Vanua Levu	-16.43	179.373
MSAPB1180-12	<i>L. (Homalictus) hadrander</i>	Fiji	Viti Levu	-17.5762	177.935
MSAPB1185-12	<i>L. (Homalictus) hadrander</i>	Fiji	Viti Levu	-17.5762	177.935
MSAPB1189-12	<i>L. (Homalictus) hadrander</i>	Fiji	Viti Levu	-17.5762	177.935
MSAPB1192-12	<i>L. (Homalictus) hadrander</i>	Fiji	Viti Levu	-17.5762	177.935
MSAPB1194-12	<i>L. (Homalictus) hadrander</i>	Fiji	Viti Levu	-17.5772	177.943
MSAPB1195-12	<i>L. (Homalictus) hadrander</i>	Fiji	Viti Levu	-17.5707	177.944
MSAPB1196-12	<i>L. (Homalictus) hadrander</i>	Fiji	Viti Levu	-17.5707	177.944
MSAPB1197-12	<i>L. (Homalictus) hadrander</i>	Fiji	Viti Levu	-17.5707	177.944
MSAPB1303-12	<i>L. (Homalictus) nr. versifrons</i>	Fiji	Viti Levu	-17.5762	177.935
MSAPB162-11	<i>L. (Homalictus) nr. versifrons</i>	Fiji	Tavueni	-16.967	179.997
MSAPB189-11	<i>L. (Homalictus) nr. versifrons</i>	Fiji	Viti Levu	-18.188	178.106
MSAPB320-11	<i>L. (Homalictus) nr. versifrons</i>	Fiji	Viti Levu	-17.595	177.967
MSAPB334-11	<i>L. (Homalictus) nr. versifrons</i>	Fiji	Viti Levu	-17.673	178
MSAPB337-11	<i>L. (Homalictus) nr. versifrons</i>	Fiji	Viti Levu	-17.678	178.001
MSAPB341-11	<i>L. (Homalictus) nr. versifrons</i>	Fiji	Viti Levu	-17.735	178.075
MSAPB342-11	<i>L. (Homalictus) nr. versifrons</i>	Fiji	Viti Levu	-17.735	178.075
MSAPB1166-12	<i>L. (Homalictus) sp. taveuni</i>	Fiji	Taveuni	-16.8287	-179.981
MSAPB1170-12	<i>L. (Homalictus) sp. taveuni</i>	Fiji	Taveuni	-16.8287	-179.981
MSAPB1171-12	<i>L. (Homalictus) sp. taveuni</i>	Fiji	Taveuni	-16.8287	-179.981
				16.967	179.997

MSAPB1183-12	<i>L. (Homalictus) versifrons</i>	Fiji	Viti Levu	-17.5762	177.935
MSAPB1304-12	<i>L. (Homalictus) versifrons</i>	Fiji	Viti Levu	-17.5762	177.935
MSAPB893-12	<i>L. (Homalictus) latro</i>	Samoa	Upolu	-13.8495	-171.759
MSAPB895-12	<i>L. (Homalictus) latro</i>	Samoa	Upolu	-13.8495	-171.759
MSAPB912-12	<i>L. (Homalictus) nr. samoae</i>	Samoa	Upolu	-13.9054	-171.796
MSAPB947-12	<i>L. (Homalictus) nr. samoae</i>	Samoa	Savaii	-13.4746	-172.404
MSAPB977-12	<i>L. (Homalictus) nr. upoluensis</i>	Samoa	Upolu	-13.5157	-172.4
MSAPB994-12	<i>L. (Homalictus) nr. upoluensis</i>	Samoa	Upolu	-13.9034	-171.795
MSAPB879-12	<i>L. (Homalictus) perpessicus</i>	Samoa	Upolu	-13.8347	-171.776
MSAPB896-12	<i>L. (Homalictus) perpessicus</i>	Samoa	Upolu	-13.8495	-171.759
MSAPB898-12	<i>L. (Homalictus) perpessicus</i>	Samoa	Upolu	-13.8495	-171.759
MSAPB905-12	<i>L. (Homalictus) perpessicus</i>	Samoa	Upolu	-13.8777	-171.948
MSAPB909-12	<i>L. (Homalictus) perpessicus</i>	Samoa	Upolu	-13.8696	-171.805
MSAPB911-12	<i>L. (Homalictus) perpessicus</i>	Samoa	Upolu	-13.9054	-171.796
MSAPB915-12	<i>L. (Homalictus) perpessicus</i>	Samoa	Upolu	-13.9054	-171.796
MSAPB921-12	<i>L. (Homalictus) perpessicus</i>	Samoa	Upolu	-14.0138	-171.608
MSAPB927-12	<i>L. (Homalictus) perpessicus</i>	Samoa	Upolu	-14.0092	-171.425
MSAPB931-12	<i>L. (Homalictus) perpessicus</i>	Samoa	Upolu	-13.8835	-171.619
MSAPB932-12	<i>L. (Homalictus) perpessicus</i>	Samoa	Upolu	-13.8835	-171.619
MSAPB937-12	<i>L. (Homalictus) perpessicus</i>	Samoa	Savaii	-13.5126	-172.302
MSAPB939-12	<i>L. (Homalictus) perpessicus</i>	Samoa	Savaii	-13.5599	-172.3
MSAPB940-12	<i>L. (Homalictus) perpessicus</i>	Samoa	Savaii	-13.5599	-172.3
MSAPB941-12	<i>L. (Homalictus) perpessicus</i>	Samoa	Savaii	-13.5599	-172.3
MSAPB942-12	<i>L. (Homalictus) perpessicus</i>	Samoa	Savaii	-13.5599	-172.3
MSAPB943-12	<i>L. (Homalictus) perpessicus</i>	Samoa	Savaii	-13.5599	-172.3
MSAPB952-12	<i>L. (Homalictus) perpessicus</i>	Samoa	Savaii	-13.4821	-172.404
MSAPB957-12	<i>L. (Homalictus) perpessicus</i>	Samoa	Savaii	-13.5751	-172.291
MSAPB958-12	<i>L. (Homalictus) perpessicus</i>	Samoa	Savaii	-13.5751	-172.291
MSAPB964-12	<i>L. (Homalictus) perpessicus</i>	Samoa	Savaii	-13.4502	-172.333
MSAPB968-12	<i>L. (Homalictus) perpessicus</i>	Samoa	Savaii	-13.5166	-172.744
MSAPB970-12	<i>L. (Homalictus) perpessicus</i>	Samoa	Savaii	-13.5166	-172.744
MSAPB986-12	<i>L. (Homalictus) perpessicus</i>	Samoa	Upolu	-13.9034	-171.795
MSAPB997-12	<i>L. (Homalictus) perpessicus</i>	Samoa	Upolu	-13.8504	-171.76
MSAPB998-12	<i>L. (Homalictus) perpessicus</i>	Samoa	Upolu	-13.8504	-171.76
MSAPB892-12	<i>L. (Homalictus) sp.</i>	Samoa	Upolu	-13.8495	-171.759
MSAPB901-12	<i>L. (Homalictus) sp.</i>	Samoa	Upolu	-13.9596	-171.857
MSAPB954-12	<i>L. (Homalictus) sp.</i>	Samoa	Savaii	-13.4821	-172.404
MSAPB866-12	<i>L. (Homalictus) stevesoni</i>	Samoa	Upolu	-13.8253	-171.773
MSAPB881-12	<i>L. (Homalictus) stevesoni</i>	Samoa	Upolu	-13.8347	-171.776
MSAPB990-12	<i>L. (Homalictus) stevesoni</i>	Samoa	Upolu	-13.9034	-171.795
MSAPB972-12	<i>L. (Homalictus) upoluensis</i>	Samoa	Savaii	-13.6303	-172.676
MSAPB983-12	<i>L. (Homalictus) upoluensis</i>	Samoa	Upolu	-13.9034	-171.795
MSAPB995-12	<i>L. (Homalictus) upoluensis</i>	Samoa	Upolu	-13.9034	-171.795
MSAPB1201-12	<i>L. (Homalictus) Solomonsi</i>	Solomon Is	Gizo	-8.1054	156.844
MSAPB694-11	<i>L. (Homalictus) aponi</i>	Vanuatu	Santo	-15.457	167.188
MSAPB838-11	<i>L. (Homalictus) aponi</i>	Vanuatu	Tanna	-19.502	169.274
MSAPB840-11	<i>L. (Homalictus) aponi</i>	Vanuatu	Tanna	-19.502	169.274
MSAPB557-11	<i>L. (Homalictus) epiensis</i>	Vanuatu	Pele	-17.498	168.419
MSAPB586-11	<i>L. (Homalictus) epiensis</i>	Vanuatu	Malekula	-16.111	167.332
MSAPB669-11	<i>L. (Homalictus) epiensis</i>	Vanuatu	Malekula	-15.892	167.226
MSAPB699-11	<i>L. (Homalictus) epiensis</i>	Vanuatu	Santo	-15.457	167.188
MSAPB774-11	<i>L. (Homalictus) epiensis</i>	Vanuatu	Santo	-15.104	167.052
MSAPB754-11	<i>L. (Homalictus) nr. epiensis</i>	Vanuatu	Santo	-15.344	167.132
MSAPB799-11	<i>L. (Homalictus) nr. epiensis</i>	Vanuatu	Santo	-15.561	166.961
MSAPB741-11	<i>L. (Homalictus) nr. ounuensis</i>	Vanuatu	Santo	-15.348	167.111
MSAPB742-11	<i>L. (Homalictus) nr. ounuensis</i>	Vanuatu	Santo	-15.348	167.111
MSAPB566-11	<i>L. (Homalictus) tannaensis</i>	Vanuatu	Malekula	-16.138	167.284
MSAPB588-11	<i>L. (Homalictus) tannaensis</i>	Vanuatu	Malekula	-16.111	167.332
MSAPB624-11	<i>L. (Homalictus) tannaensis</i>	Vanuatu	Malekula	-15.95	167.182
MSAPB631-11	<i>L. (Homalictus) tannaensis</i>	Vanuatu	Malekula	-15.95	167.182
MSAPB634-11	<i>L. (Homalictus) tannaensis</i>	Vanuatu	Malekula	-15.95	167.182
MSAPB682-11	<i>L. (Homalictus) tannaensis</i>	Vanuatu	Santo	-15.457	167.188
MSAPB718-11	<i>L. (Homalictus) tannaensis</i>	Vanuatu	Santo	-15.449	167.2
MSAPB722-11	<i>L. (Homalictus) tannaensis</i>	Vanuatu	Santo	-15.449	167.2
MSAPB804-11	<i>L. (Homalictus) tannaensis</i>	Vanuatu	Santo	-15.556	166.95
MSAPB821-11	<i>L. (Homalictus) tannaensis</i>	Vanuatu	Tanna	-19.528	169.262
MSAPB519-11	<i>L. (Homalictus) wilsoni</i>	Vanuatu	Efate	-17.557	168.461
MSAPB703-11	<i>L. (Homalictus) zingowli</i>	Vanuatu	Santo	-15.451	167.187
MSAPB706-11	<i>L. (Homalictus) zingowli</i>	Vanuatu	Santo	-15.451	167.187
				15.407	167.11

MSAPB752-11	<i>L. (Homalictus) zingowli</i>	Vanuatu	Santo	-15.344	167.132
MSAPB773-11	<i>L. (Homalictus) zingowli</i>	Vanuatu	Santo	-15.104	167.052
MSAPB793-11	<i>L. (Homalictus) zingowli</i>	Vanuatu	Santo	-15.561	166.961
MSAPB794-11	<i>L. (Homalictus) zingowli</i>	Vanuatu	Santo	-15.561	166.961

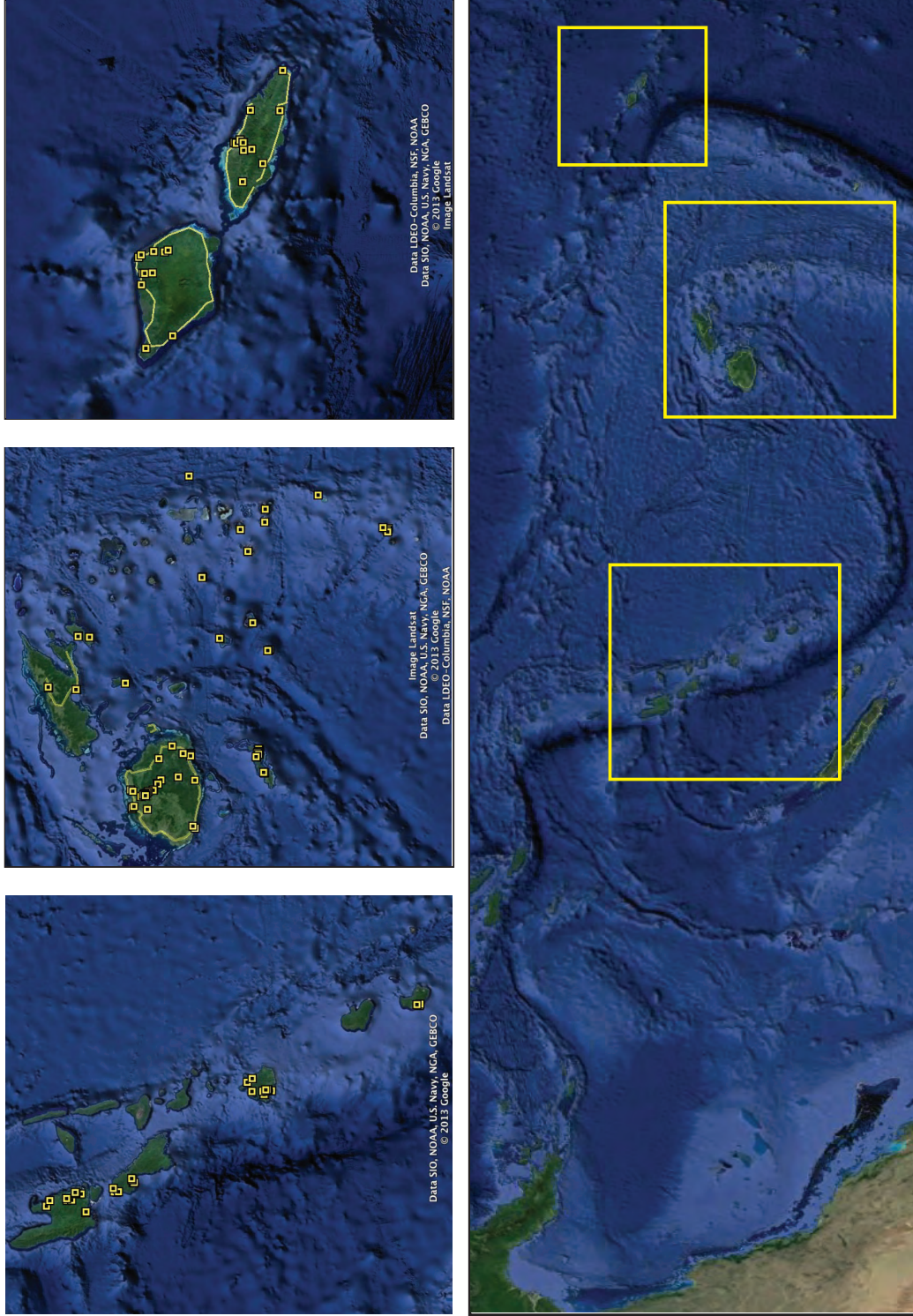


Figure S1. Collecting sites from Vanuatu, Fiji, and Samoa, for all included specimens. Highlighted squares correspond to inset maps for each archipelago

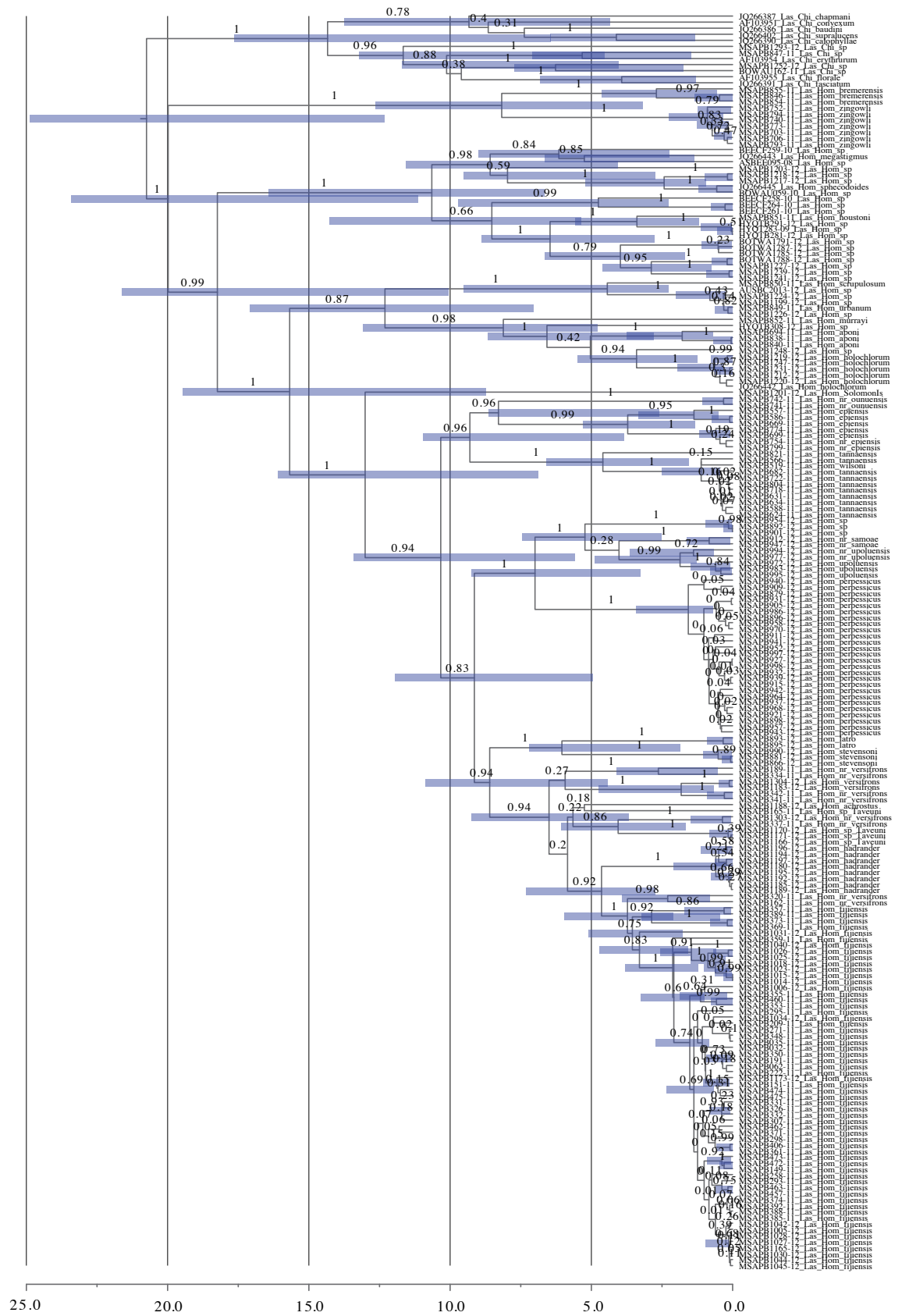


Figure S2. Bayesian chronogram produced with BEAST using an uncorrelated log-normal relaxed clock, GTR+I+ Γ substitution and Yule Process speciation models. Error bars and maximum credibility values are provided for each node. Time scale provided in millions of years with root height prior set to mean of 20 Mya based on Gibbs et al. (2012). Either BOLD ID number or Genbank Accession numbers are provided with genus and subgenus names shortened as follows: *Lasioglossum* (Las), *Chilalictus* (Chi), and *Homalictus* (Hom).

Figure S3. Genetic distance based neighbour-joining cladogram. Numbers above nodes indicate where bootstrap support values were not strong (*i.e.* >90). BOLD ID or Genbank Accession numbers provided with genus and subgenus names shortened as follows: *Lasioglossum* (Las), *Chilalictus* (Chi), and *Homalictus* (Hom).

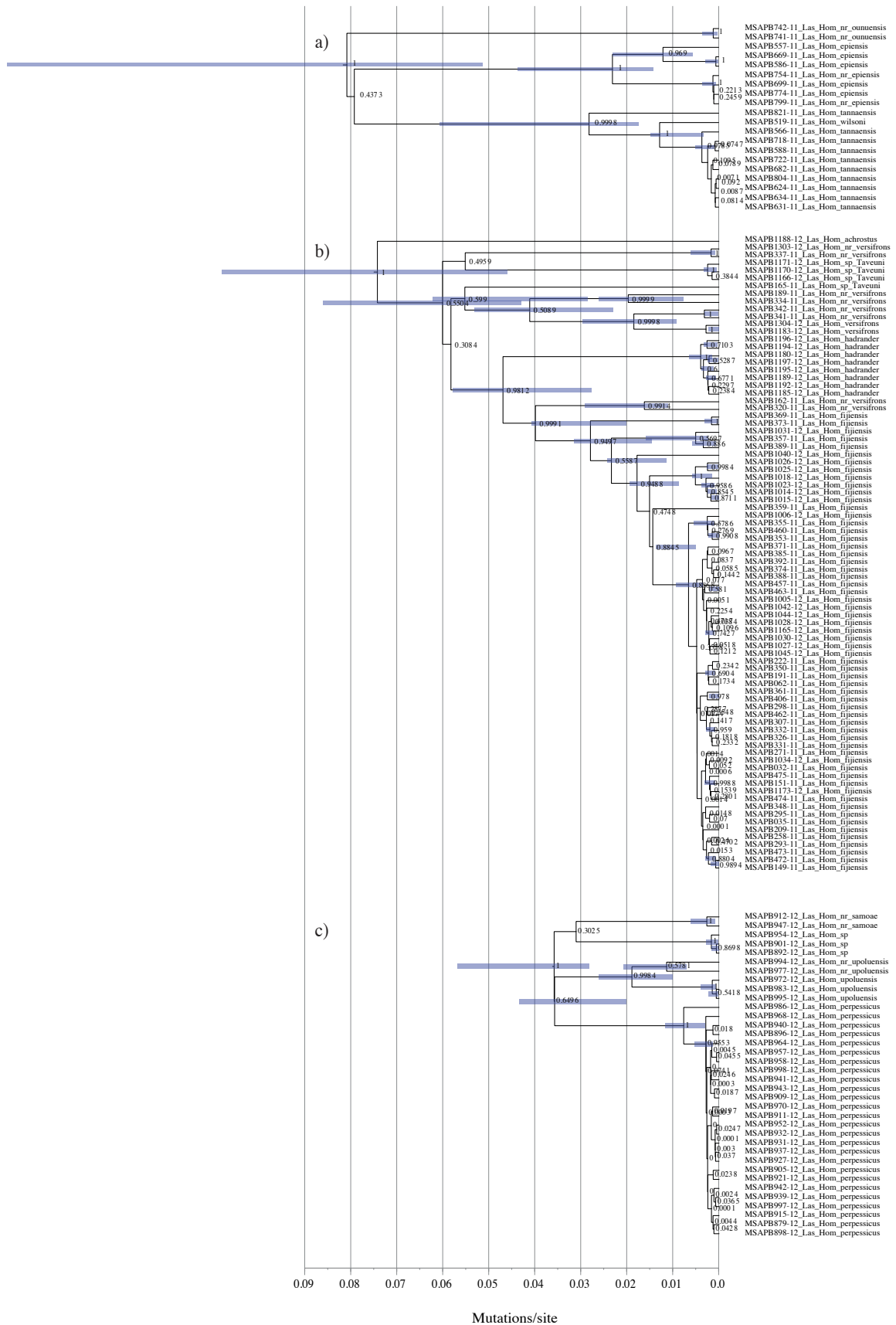
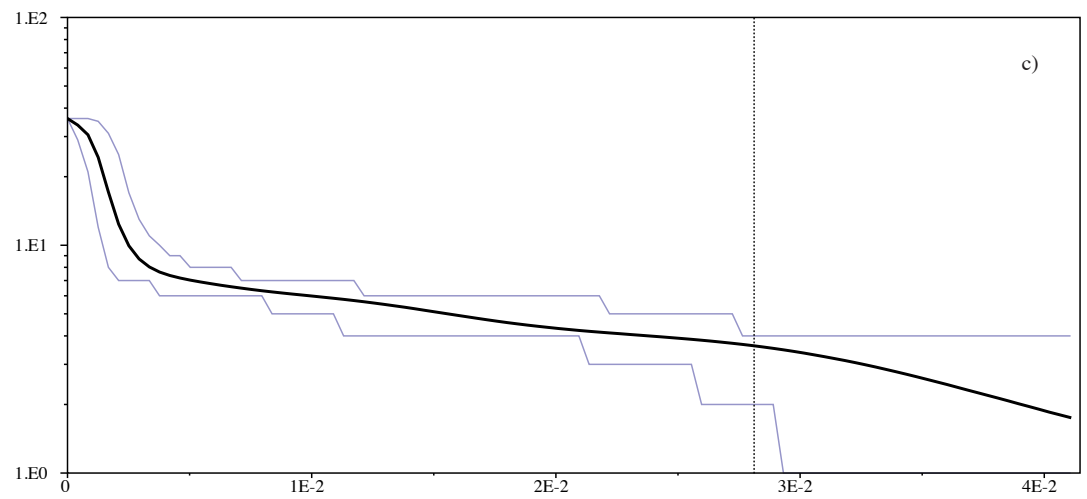
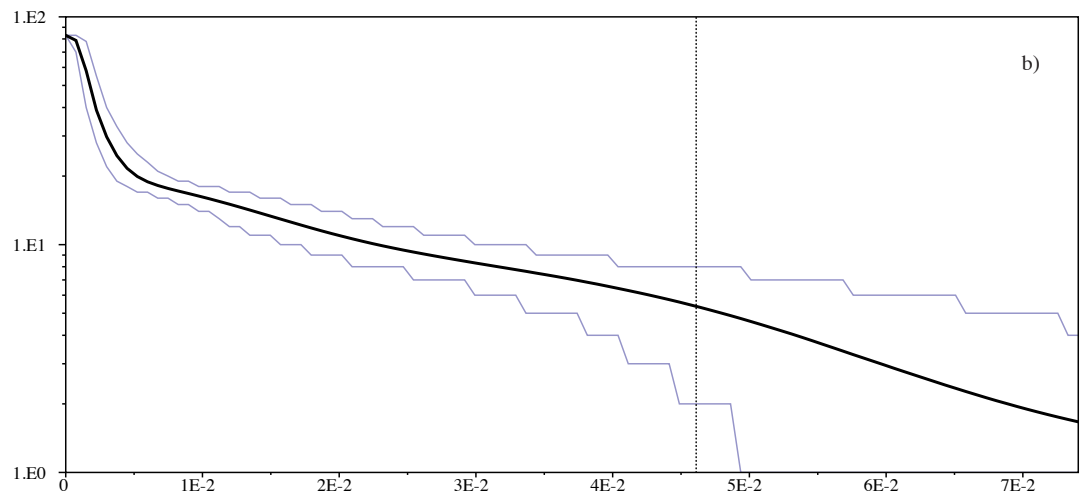
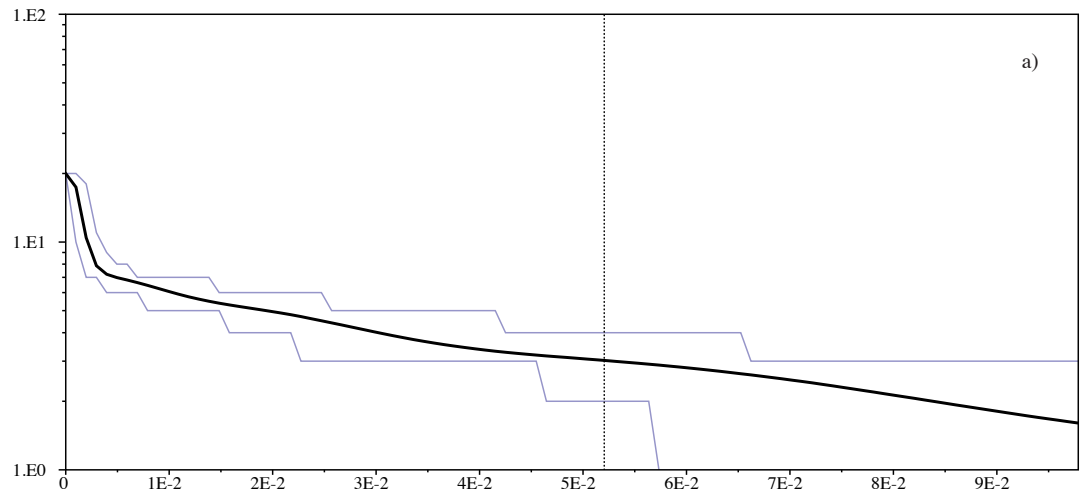


Figure S4. Maximum credibility trees implemented via BEAST with a strict molecular clock, fixed to 1.0, and Bayesian skyline speciation model. Maximum credibility values are provided for each node, as are confidence bars. Scale given in units of mutations per site. Trees represent archipelagos as follows: a) Vanuatu, b) Fiji, c) Samoa.



Mutations/site

Figure S5. Log lineage through time (LTT) plots for each of the Pacific archipelagos based on Bayesian skyline chronograms following a burnin of 10% with an enforced strict clock rate of 1.0 implemented in Tracer. X-axis given in units of mutations per site. Plots represent archipelagos as follows: a) Vanuatu, b) Fiji, c) Samoa.

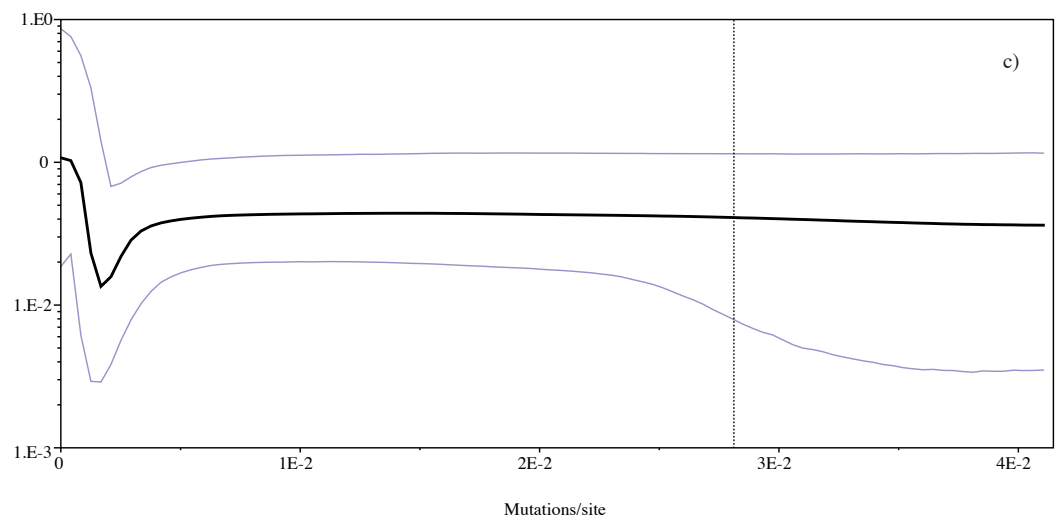
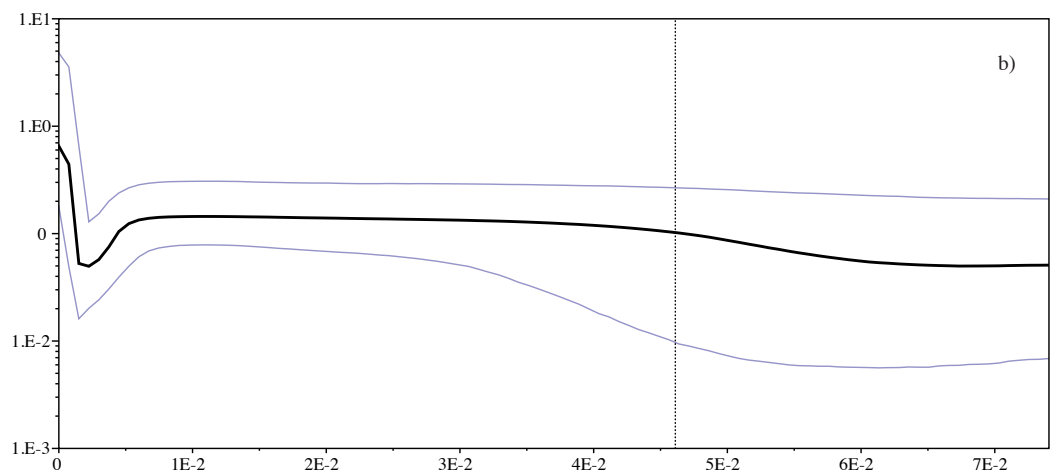
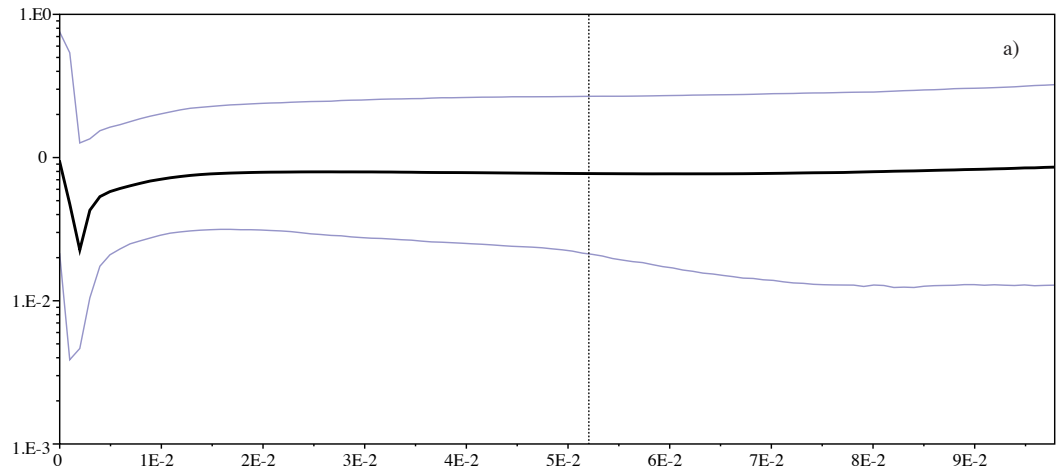


Figure S6. Bayesian sky plot (BSP) for each of the archipelagos based on a strict clock analysis with an enforced strict clock rate of 1.0 implemented in Tracer. The bold black line indicates the mean plot values and the shaded area represents upper and lower confidence intervals for mean estimates. The y-axis can be interpreted as N_e mutation rate/site, and if mutations rates are assumed to be constant, this can be interpreted as a measure of relative N_e over time. The x-axis is given in units of mutations per site. Plots represent archipelagos as follows: a) Vanuatu, b) Fiji, c) Samoa.